



# Discovery of *N*-(6-(5-fluoro-2-(piperidin-1-yl)phenyl)pyridazin-3-yl)-1-(tetrahydro-2H-pyran-4-yl)methanesulfonamide as a brain-permeable and metabolically stable kynurenine monooxygenase inhibitor

Katsunori Tsuboi, Hidenori Kimura, Yoshie Nakatsuji, Momoe Kassai, Yoko Deai, Yoshiaki Isobe\*

Drug Research Division, Sumitomo Dainippon Pharma. Co., Ltd., 3-1-98, Kasugade-naka, Konohana-ku, Osaka 554-0022, Japan

## ARTICLE INFO

### Keywords:

Kynurenine monooxygenase  
KMO  
Kynurenine pathway  
Huntington's disease  
KYNA  
3-HK  
Brain permeable  
BBB  
R6/2

## ABSTRACT

Kynurenine monooxygenase (KMO) is expected to be a good drug target to treat Huntington's disease (HD). This study presents the structure-activity relationship of pyridazine derivatives to find novel KMO inhibitors. The most promising compound **14** resolved the problematic issues of lead compound **1**, i.e., metabolic instability and reactive metabolite-derived side-effects. Compound **14** exhibited high brain permeability and a long-lasting pharmacokinetics profile in monkeys, and neuroprotective kynurenic acid was increased by a single administration of **14** in R6/2 mouse brain. These results demonstrated **14** may be a potential drug candidate to treat HD.

Huntington's disease (HD) is a genetic neurodegenerative condition caused by a CAG repeat expansion in the huntingtin gene, and is a dominantly inherited progressive neurological disorder and presents a combination of motor, cognitive, and psychiatric problems that progress over a 20-year period until death.<sup>1</sup> Tetraabenazine is a dopamine-depleting agent that is effective for reducing chorea, although it risks potentially serious adverse effects as depression, suicide, and cardiotoxicity. Furthermore, tetraabenazine is a symptomatic therapy, and the disease modifying agents are not available in clinic. Similar to drug development for other neurological diseases, failure rates in HD drug development remain high.<sup>2</sup>

The kynurenine pathway (KP) is the major route for tryptophan metabolism in mammals and produces neuroactive metabolites. KP metabolite imbalances lead to elevated levels of the free-radical generator 3-hydroxykynurenine (3-HK) and the excitotoxin quinolinic acid (QA) relative to the neuroprotective metabolite kynurenic acid (KYNA), contributing to the pathogenesis of HD.<sup>3,4</sup> Early-stage HD patients have an increased 3-HK/KYNA ratio in the striatum and cortex compared with healthy controls.<sup>5</sup> The downregulation of kynurenine monooxygenase

(KMO) activity shifts the flux between the two branches of the KP toward increased KYNA formation, thus generating a neuroprotective environment (Fig. 1). KMO inhibitors can correct the 3-HK/KYNA imbalance in HD patients and are therefore considered in strategies to prevent or arrest neurodegeneration.

A number of KMO inhibitors have been reported, but no compounds have entered into clinical development.<sup>6</sup> All compounds in Fig. 2 contain an acidic functional group as a common feature. The acidic compounds carry a negative charge at physiological pH, making it difficult for them to cross the blood-brain barrier (BBB). Ro-61-8048 demonstrated KMO inhibition both *in vitro* and *ex vivo*, but its efficacy in the brain was poorer than that in the liver.<sup>7</sup> We also confirmed the brain penetration of Ro-61-8048 and CHDI340236 in a mouse pharmacokinetic (PK) study, but their brain penetration was <1%, indicating negligible brain exposure. Zwilling *et al.* reported that JM-6, a non-brain permeable KMO inhibitor, was effective at regulating brain kynurenine metabolism.<sup>8</sup> However, the PK/PD relationship was unclear, since the KMO inhibition by JM-6 was very weak (IC<sub>50</sub> = 20 μM) and JM-6 was metabolically unstable.<sup>9</sup> We previously reported compound **1** as a brain

\* Corresponding author.

E-mail address: [yoshiaki-isobe@ds-pharma.co.jp](mailto:yoshiaki-isobe@ds-pharma.co.jp) (Y. Isobe).

<https://doi.org/10.1016/j.bmcl.2021.128115>

Received 26 March 2021; Received in revised form 4 May 2021; Accepted 13 May 2021

Available online 17 May 2021

0960-894X/© 2021 Elsevier Ltd. All rights reserved.

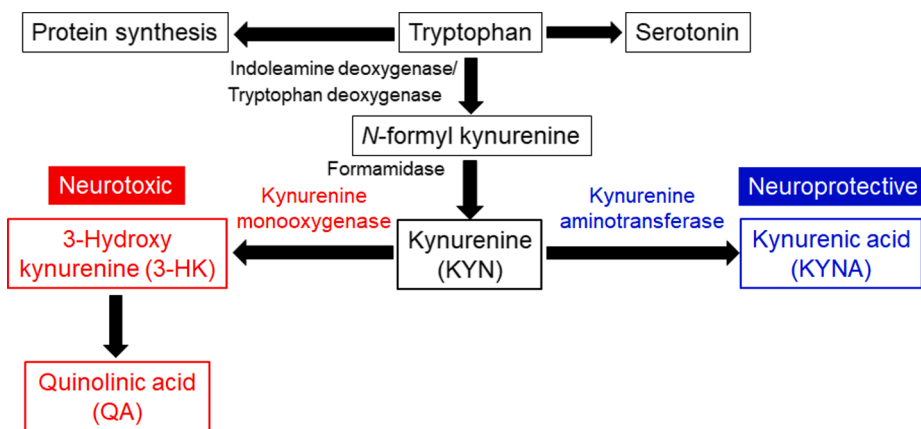


Fig. 1. Kynurenine pathway of tryptophan metabolism.

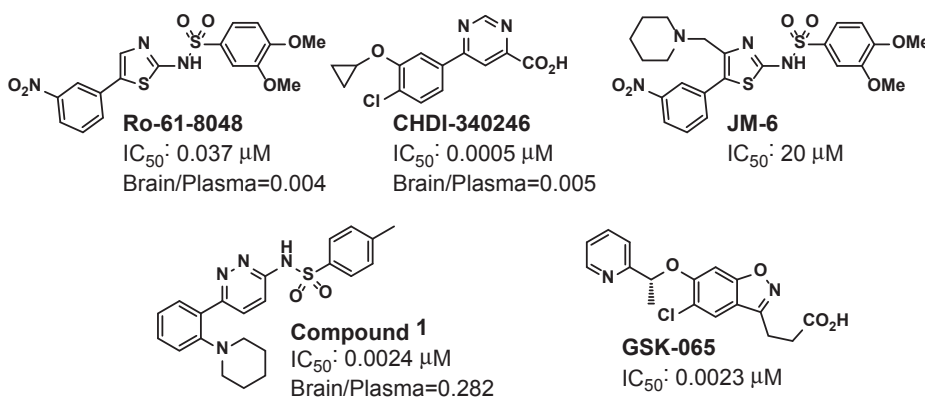


Fig. 2. Chemical structures of known KMO inhibitors and compound 1.

permeable and strong KMO inhibitor: its  $IC_{50}$  toward human KMO (hKMO) was 2.4 nM, and the mouse PK study indicated its brain/plasma concentration ratio was 0.282, much higher than the ratios of Ro-61-8048 and CHDI-340246.<sup>10</sup> Compound 1 corrected the 3-HK/KYNA imbalance in the brain striatum and improved the cognition impairment in R6/2 mice by oral administration, but the improvement of motor function was not statistically significant. We hypothesized that observation of the long-lasting PK profile is required to show potent *in vivo* efficacy.

Detailed evaluation of the drug metabolism and PK revealed that compound 1 has two problematic issues to be resolved. First is that compound 1 is not metabolically stable: its intrinsic clearance is 1.07  $\mu\text{L}/\text{min}/\text{mg}$  protein for human and 0.395  $\mu\text{L}/\text{min}/\text{mg}$  protein for rat following incubation with hepatic microsomes and NADPH at 37 °C for 30 min. We concluded that this instability profile led to the short plasma half-life ( $T_{1/2} = 0.3$  h) of 1 in the above mouse PK study. The second issue is that compound 1 risks the formation of reactive metabolites. Reactive metabolites have been putatively linked to drug-related side effects including liver dysfunction, agranulocytosis, and aplastic anemia, *etc.* Dansylated glutathione (dGSH) has been used as a trapping agent for the quantitative estimation of reactive metabolites.<sup>11</sup> Compound 1 was incubated with dGSH and human hepatocyte microsomes, and the amount of compound 1-dGSH conjugate was measured using a fluorescence detector and HPLC analysis. High dGSH-conjugate formation was seen in compound 1 (0.852  $\mu\text{mol}/\text{L}$ ). In order to improve both the metabolic stability and reactive metabolite formation, we planned the following optimization strategy. The electron-rich benzene ring often becomes the target site for CYP enzyme metabolism and dGSH-conjugate formation. In general, a high degree of correlation between the lipophilicity and metabolism is seen in drug discovery.<sup>12</sup> Thus, based

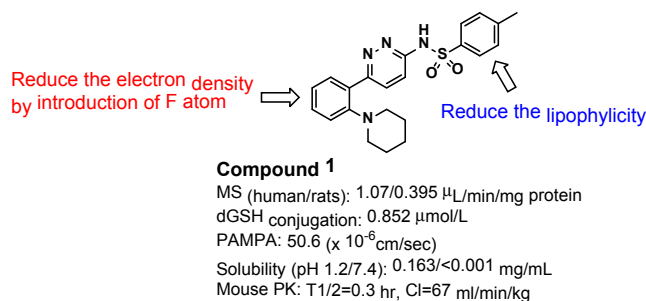
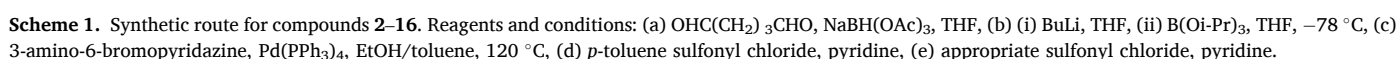


Fig. 3. DMPK profile of compound 1 and optimization strategy.

on 1, we planned to introduce a fluorine (F) atom at the phenyl moiety to reduce the electron density and to replace the toluoyl group with a low-lipophilic one to resolve the two issues (Fig. 3).

The synthetic route of pyridazine derivatives is shown in Scheme 1. The reductive amination of commercially available 2-bromoaniline (A1-4) and glutaraldehyde, followed by the reaction with triisopropyl borate gave boronate (B1-4). Suzuki-Miyaura coupling of the boronate with 3-amino-6-bromopyridazine in the presence of  $\text{Pd}(\text{PPh}_3)_4$  afforded a pyridazine intermediate (C1-4). Subsequently, the reaction of (C1-4) with *p*-toluene sulfonyl chloride in pyridine gave targets 2-5 in moderate yields. Compounds 6-16 were prepared by the reaction of C-2 with the appropriate sulfonyl chloride in pyridine. The compound screening was carried out by the hKMO assay: the mitochondrial fraction of human liver was pre-incubated with the test compounds for 5 min, *L*-kynurenine was added and incubated for 30 min, and then the amount of generated 3-HK (converted from *L*-kynurenine by hKMO) was measured by LC/MS/

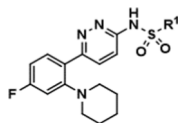
C1=CC=C(S(=O)(=O)NC2=CC=CC=C2)C=C1C3=CC=CC=C3N4CCCCC4

a:  $\mu\text{L}/\text{min}/\text{mg}$  protein, b:  $\text{ng}/\text{mL}$ , c:  $\text{ng}/\text{g}$  tissue, d:  $10 \text{ mg}/\text{kg}$ , po.

First, we introduced a F atom onto the phenyl moiety of **1** to reduce the electron density. The results are summarized in [Table 1](#). Compounds **3–5** showed single nM level potencies toward hKMO, but the IC<sub>50</sub> of **2** was 20 nM, approximately 8-fold weaker than **1**, suggesting the 3rd position was unfavorable in terms of hKMO inhibition. The reduction of electron density of phenyl group by F atom was often effective to improve microsomal stability (MS) in drug discovery.<sup>13</sup> Human MS was significantly improved by all compounds, as we expected, but rat MS was not. Introduction of the F atom at the 3<sup>rd</sup> or 4<sup>th</sup> position was effective at reducing the conjugate formation by compounds **2** and **3** but not for compounds **4** and **5**. Unfortunately, it was difficult to understand these results from the view point of electron density. We evaluated the brain permeability of test compounds **3–5** by a mouse PK study, finding that the brain/plasma concentration ratios of the compounds were similar to that of compound **1**, indicating the F atom did not influence on brain permeability. Considering a balance of hKMO inhibition, human/rat MS, and the dGSH conjugate, the 4th position could be considered best for introduction of the F atom. The biological profile of **3** is superior to compound **1**; however, further improvement in the MS is needed to obtain long-lasting compounds. Compound **3** is a lipophilic compound (clogP = 4.4). Therefore, we speculated that further reduction of the lipophilicity may be useful to improve the MS. Accordingly, we explored optimization at the toluoyl moiety in compound **3** (see [Table 2](#)).

We replaced the toluoyl moiety in **3** with an alkyl group. The hKMO inhibitory activity of ethyl (**6**) was 115 nM, approximately 13-fold weaker than **3**, but the inhibitory activity was enhanced by the alkyl chain elongation: propyl (**7**: 37 nM), isobutyl (**8**: 27 nM), cyclopentylmethyl (**9**: 29 nM). On the other hand, human MS may also correlate with lipophilicity, and clogP should be <3.5 to obtain metabolically stable compounds. Interestingly, the hKMO inhibitory activity of trifluoroethyl (**10**) was 3-fold stronger than **6**, suggesting the acidity is important for hKMO inhibition. In contrast, the human MS worsened with **10**, because the lipophilicity of **10** was higher than of **6**. In order to reduce the lipophilicity (clogP: <3) we designed and prepared ether-type compounds (**11** and **12**), finding they had favorable human MS but not strong hKMO inhibition. The results of **6**–**12** suggested that it is difficult to balance good human MS and hKMO inhibition. The results of compounds **9** and **12** led us to prepare a cyclic ether analogue (**13**). The human/rat MS of **13** was much improved compared with **9** while maintaining the hKMO inhibitory activity. Thus, we investigated cyclic ether analogues (**14**–**16**) and identified compound **14** with the best balance. Although the hKMO inhibitory activity of **14** was 5-fold weaker than **1**, compound **14** showed good human/rat MS. Furthermore, the d-GSH-conjugate formation of **14** was much lower than **1**, suggesting **14** was a low-risk compound in terms of reactive metabolite-derived side-effects. Therefore, compound **14** can be considered a candidate that resolves the problematic issues of **1**.

**Table 2**  
SAR exploration of compounds 6–16.



Compound	R <sup>1</sup>	hKMO IC <sub>50</sub> (nM)	clogP	microsomal stability <sup>a</sup>		dGSH (μmol/ L)
				human	rats	
3	4-Me-Ph	9.1	4.4	0.41	0.272	0.073
6	Et	115.5	3.01	0.156	<0.05	0
7	<i>n</i> -Pr	37.1	3.54	0.179	0.168	0
8	<i>i</i> -Bu	27.2	3.94	0.375	0.483	0.11
9	CH <sub>2</sub> -c-Pen	28.6	4.57	0.703	1.6	0.49
10	CH <sub>2</sub> CF <sub>3</sub>	38.7	3.28	0.569	0.265	0
11	(CH <sub>2</sub> ) <sub>2</sub> OMe	83.9	2.6	0.179	0.05	0
12	(CH <sub>2</sub> ) <sub>3</sub> OMe	61.6	2.98	0.026	0.045	0
13		41	3.1	0.179	0.086	0.289
14		12.8	2.73	0.068	0.218	0.092
15		17.9	2.73	0.081	0.23	nt <sup>b</sup>
16		34.1	3.53	0.139	0.435	0
Ro-61-8048		33.8	3.23	0.49	<0.05	0.22

a: μL/min/mg protein, b: nt means not tested.

The PK profile of compound **14** was characterized in cynomolgus monkeys. Compound **14** demonstrated good clearance (8.0 mL/min/kg) with a favorable plasma half-life of 6.2 h when intravenously administered. Compound **14** also exhibited good oral exposure (BA = 25%) and a long-lasting profile when dosed orally, as shown in Fig. 4. In order to be an effective neuroprotective agent for HD treatment, a compound

should be able to cross the BBB to reach the target tissue. We tested the brain permeability of **14** in cynomolgus monkeys. Blood and brain samples were collected two hours after the oral dosing of **14**. As shown in Table 3, compound **14** exhibited good brain penetration, and the striatum/plasma concentration ratio reached 0.43. In addition, we tested the brain permeability of CHDI-340246 as a reference. The plasma concentration of CHDI-340246 was very high by oral administration, but the striatum/plasma ratio was only 0.04, 100-fold lower than that of compound **14**.

R6/2 transgenic mice are a well-characterized animal model mimicking many of the histopathological aspects of HD.<sup>14</sup> In R6/2 mice, motor symptoms, such as dyskinesia, ataxia, and clasp behavior, start at the age of 6 weeks. From the age of 9–10 weeks, the mice show significant neuronal dysfunction and display neuronal atrophy in the striatum.<sup>15</sup> An increase in 3-HK levels was also reported in the brains of R6/2 mice.<sup>16,17</sup> We tested the efficacy of **14** on the localization of KP-metabolites in R6/2 mice. Compound **14** was orally dosed in 8-week-old R6/2 mice. The amount of KP metabolites in the striatum was measured at 1 h after the dosing. The results are summarized in Fig. 5. Although the level of neurotoxic 3-HK did not change with the dose, neuroprotective KYNA was increased >10-fold in a dose-dependent manner. Thus, the 3-HK/KYNA ratio was improved, indicating a neuroprotective environment. In another experimental, 45% reduction of 3-HK by **14** administration (100 mg/kg, po) was observed at 24 h after dosing. This result suggested the half-life of 3-HK in brain might be long, and we speculated that repeated administration is required to show clear 3-HK reduction in brain. Our pharmacology colleagues have a plan to test **14** on the motor/cognition functions and histopathological findings of R6/2 mice by repeated administration, and the detail results will be reported in the future.

In conclusion, we investigated brain-permeable KMO inhibitors with long-lasting PK profiles for the treatment of HD. We conducted an optimization study based on compound **1**. The introduction of an F atom onto the 3rd position of the phenyl moiety improved human MS and d-GSH-conjugate formation. Replacement of the toluoyl moiety in **3** with a

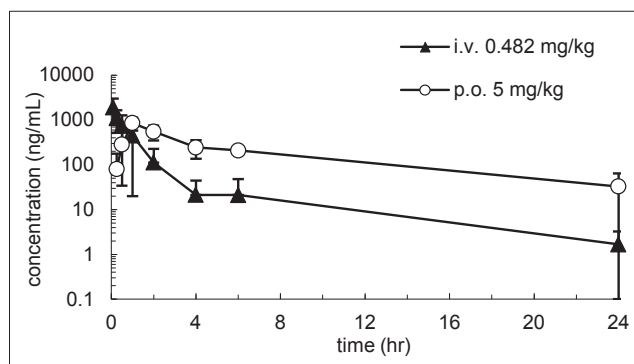


**Fig. 4.** Plasma concentration curve of **14** in cynomolgus monkeys.

**Table 3**  
Striatum/plasma concentration ratio of **14** and CHDI-340246 in cynomolgus monkeys.

Compound	Time (hr)	Animal No.	Plasma (ng/mL)	Striatum (ng/g)	Striatum/Plasma Ratio
<b>14</b>	2	1	873	318	0.36
		2	1930	940	0.49
		Mean	1402	629 (24 nM <sup>a</sup> )	0.43
CHDI-340246	2	1	14,200	56.0	0.004
		2	17,000	73.5	0.004
		Mean	15,600	64.8	

a) Brain free concentration (protein binding ratio = 98.4%).

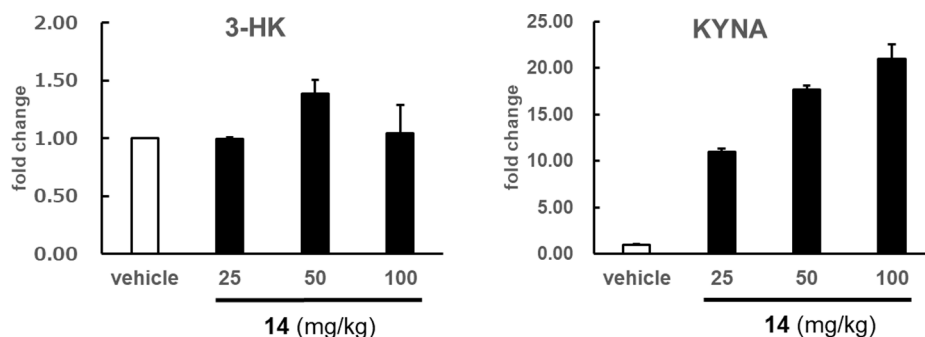


Fig. 5. 3-HK and KYNA concentrations in R6/2 mice brain.

cyclic ether group further improved human and rat MS. As a result of the optimization, we succeeded to identify compound **14** as a well-balanced compound in terms of hKMO inhibition, human/rat MS, and dGSH-conjugate formation. A cynomolgus monkey PK study indicated that **14** has good brain permeability with a long-lasting profile and was superior to CHDI-340246 in terms of brain penetration. Neuroprotective KYNA was significantly increased in R6/2 mouse brain by a single administration of **14**. Overall, compound **14** resolved the problematic issues of **1** and is expected to be drug candidate for HD treatment.

#### Declaration of Competing Interest

The authors declare that they have no known competing financial interests or personal relationships that could have appeared to influence the work reported in this paper.

#### Acknowledgement

The authors would like to thank Ms. Mari Miyajima, Mr. Itaru Natutani and Dr. Kazuto Yamada for their technical support and useful advice.

#### Appendix A. Supplementary data

Supplementary data to this article can be found online at <https://doi.org/10.1016/j.bmcl.2021.128115>.

#### References

- Bachoud-Lévi AC, Ferreira J, Massart R, et al. *Front Neurol*. 2019;10:710.
- Caron NS, Dorsey ER, Hayden MR. *Nat Rev Drug Discovery*. 2018;17:729–750.
- Maddison DC, Giorgini F. *Semin Cell Dev Biol*. 2015;40:134–141.
- Chen Y, Guillemin GJ. *Int J Trp Res*. 2009;2:1–19.
- Schwarz MJ, Guillemin GJ, Teipel SJ, Buerger K, Hampel H. *Eur Arch Psychiatry Clin Neurosci*. 2013;263:345–352.
- Zhang S, Sakuma M, Deora GS, et al. *Commun Biol* 2019;2:271–271.
- Rover S, Cesura AM, Huguenin P, Kettler R, Szente A. *J Med Chem*. 1997;40:4378–4385.
- Zwilling D, Huang SY, Sathyaikumar KV, et al. *Cell*. 2011;145:863–874.
- Beconi MG, Yates D, Lyons K, et al. *Drug Metab Dispos*. 2012;40:2297–2306.
- Kimura H, Suda H, Kassai M, et al. *Bioorg Med Chem Lett*. 2021;33, 127753.
- Attwa MW, Kadi AA, Abdelhameed AS. *J Separation Sci*. 2020;43:708–718.
- Waring MJ. *Expert Opin Drug Discov*. 2010;5:235–248.
- Clader JW. *J Med Chem*. 2004;47:1–9.
- Mangiarini L, Sathasivam K, Seller M, et al. *Cell*. 1996;87:493–506.
- Stack EC, Kubilius JK, Smith K, et al. *J Comp Neurol*. 2005;490:354–370.
- Guidetti P, Bates GP, Graham RK, et al. *Neurobiol Dis*. 2006;23:190–197.
- Sathyaikumar KV, Stachowski EK, Amori L, Guitti P, Muchowski PJ, Schwarcz R. *J Neurochem*. 2010;113:1416–1425.